Received: 25 January 2022 | Revised: 9 May 2023 | Accepted: 10 December 2023

DOI: 10.1002/rnc.7150

RESEARCH ARTICLE

WILEY

Fixed-time integral sliding mode control for admittance control of a robot manipulator

Yuzhu Sun[1] | **Mien Van**[1] | **Stephen McIlvanna**[1] | **Seán McLoone**[1] | **Dariusz Ceglarek**[2]

[1]School of Electronics, Electrical and Computer Science, Queen's University Belfast, Belfast, UK

[2]Warwick Manufacturing Group, University of Warwick, Coventry, UK

Correspondence
Mien Van, School of electronics, electrical and computer science, Queen's University of Belfast, Belfast BT7 1NN, UK.
Email: M.Van@qub.ac.uk

Funding information
Natural Environment Research Council, Grant/Award Number: NE/V008080/1; Royal Society, Grant/Award Numbers: IEC/NSFC/211236, RGS/R1/221356; U.K. EPSRC Made Smarter Innovation (MSI) - Research Centre for Smart, Collaborative Industrial Robotics, Grant/Award Number: EP/V062158/1

Abstract

This article proposes a novel fixed-time integral sliding mode controller for admittance control to enhance physical human-robot collaboration. The proposed method combines the benefits of compliance to external forces of admittance control and high robustness to uncertainties of integral sliding mode control (ISMC), such that the system can collaborate with a human partner in an uncertain environment effectively. First, a fixed-time sliding surface is applied in the ISMC to make the tracking error of the system converge within a fixed time regardless of the initial condition. Then, a fixed-time backstepping controller (BSP) is integrated into the ISMC as the nominal controller to realize global fixed-time convergence. Furthermore, to overcome the singularity problem, a nonsingular fixed-time sliding surface is designed and integrated into the controller, which is useful for practical application. Finally, the proposed controller is validated for a two-link robot manipulator with uncertainties and external human forces. The results show that the proposed controller is superior in the sense of both tracking error and convergence time, and at the same time, can comply with human motion in a shared workspace.

KEYWORDS

admittance control, fixed-time convergence, Integral sliding mode control, physical human-robot collaboration, robot manipulator

1 | INTRODUCTION

Recent developments in biomedical, social and industrial robotics have led to an increasing interest in the field of physical human-robot collaboration (pHRC).[1,2] Robots that can physically collaborate with human partners enable the cognitive strengths of humans and the high-precision and repeatability of robots to be combined. Unlike fully automated industrial production lines, to effectively work with the human partner in a shared workspace involving activities such as object handovers or co-carrying, it is imperative that the cooperative robots are capable of simultaneously complying with human forces at the contact point rather than rejecting them as external disturbances.[3] Therefore, impedance/admittance control based compliance control strategies have been attracting significant interest for this application. These include the adaptive admittance control,[4] adaptive impedance control,[5,6] and robust impedance control[7,8] and so forth.

Consider an industrial robot that is required to work with a human partner in an uncertain environment. The controller of the robot should be capable of tracking a certain trajectory with external uncertainties and perturbations, and at

the same time, be compliant with human forces without the loss of stability. A considerable literature exists on techniques for improving the tracking performance of robot manipulators in an uncertain environment. For many years, model-free control strategies such as PID have been extensively employed in industrial robots.[9] However, PID has limited ability to against uncertainties and disturbances which are inevitable in the real-life robot application. Therefore, from a practical standpoint, robust control methods have emerged and been widely studied in the field of robotics to provide robustness against the effects of parametric uncertainties and external disturbances.[10] Sliding mode control (SMC) has been one of the most well-known robust control methods. However, the implementation of SMC could be problematic because the tuning of parameters is challenging. The system response is hard to predict since the controller parameters affect it in a complicated manner.[11] Additionally, the SMC scheme involves (i) the reaching phase, in which the system converges from the initial state to the sliding surface, and (ii) the sliding phase, in which the system has reached the sliding surface and tries to stay on the equilibrium point. However, the effectiveness of SMC is limited by the reaching phase which is sensitive to disturbances. Therefore, to overcome the limitation of SMC, integral sliding mode control (ISMC) has been developed. ISMC eliminates the reaching phase by finding a suitable initial position to reject disturbances from the early beginning, which is helpful for practical applications.[10] In addition, the integral term of ISMC provides one more degree of freedom for the control design to achieve more desired specifications.

Furthermore, the settling time is one of the most important properties of the time-critical system.[12] Small settling time means fast tracking-error convergence and higher robustness, which accords with real-world application requirements. The settling time of traditional finite-time control strategies[13,14] depends on the initial conditions of the system, which limits its practical application because the initial conditions are not always available as a priori. The fixed-time type controller does not depend on the initial conditions with the result that the convergence time can be determined a priori based on the design parameters.[14] This provides a solution for the limitation of traditional SMC. The performance of the system response could be more predictable in the real implementation. Therefore, to obtain the property of fast tracking-error convergence, a further extension of ISMC, called fixed-time integral sliding mode control (FTISMC),[15–17] which incorporates the benefits of ISMC and fixed-time sliding mode control (FxTSMC)[18] has been proposed. In the work of Huang and Wang,[15] a FTISMC is proposed that stabilizes a highly complex nonlinear system within a fixed time and effectively restrains the irregular and nonlinear vibrations of the system. In the work of Li et al.[16] a new integral high-order sliding mode controller is proposed for high-order nonlinear systems with fixed-time convergence. In addition, the singularity problem always comes up in the sense of fixed-time stability when calculating the derivative of sliding variables. To address this issue, several approaches have been developed to avoid or eliminate the singularity.[9,19–22] In the work of Feng et al.[19] a global nonsingular terminal sliding mode controller is presented for second-order systems to overcome the singularity problem. In the work of Zuo,[21] a new sliding surface is proposed to circumvent the singularity problem. In the work of Van and Ceglarek,[22] a new fault-tolerant control scheme based on a nonsingular fixed-time sliding mode controller is proposed for robot manipulators, which guarantees a global fixed-time convergence. Nonsingularity is essential for fixed-time control to avoid generating unbounded control input, which is undesirable in practice.

So far there is a little control method that considers compliance, robustness and fast tracking-error convergence for physical human-robot collaboration. According to the above discussion, the admittance control can provide smoother, softer motions for the robot to comply with human forces during the pHRC, and the fixed-time control processes have some good properties such as robustness and fast tracking-error convergence. Moving along these lines, this article proposes a new FTISMC control scheme for admittance control of a robot manipulator, as depicted in Figure 1. The proposed control strategy provides a solution for the contact-rich pHRC, which achieves both compliance and robustness when external human forces are applied. Furthermore, for ease of practical application, a nonsingular fixed-time integral sliding mode controller is designed. The proposed method is then simulated on a two-link robot manipulator and compared with other state-of-the-art control strategies. The simulation results show that the proposed controller is superior in the sense of robustness and convergence time. The contributions and innovations of the proposed approach can be highlighted in a comparison with other approaches as follows:

1. The existing control methods for traditional automated robots, which track their pre-defined task trajectory as accurately as possible, will reject human forces as disturbances. Such control methods conflict with the objective of physical human-robot collaboration which requires the robot to be capable of adapting human motion by complying with human contact forces. The proposed approach considers both compliance and robustness of the controller when human forces are applied. On the one hand, robots could perform more human-friendly behaviors during force interaction, and on the other hand, better tracking performance and robustness are obtained without the loss of stability with the presence of external human forces and uncertainties. The flexibility, adaptability and robustness of the

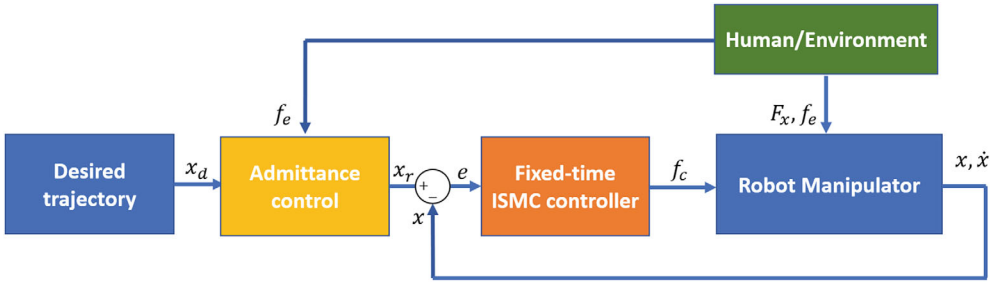

FIGURE 1 Structure of the proposed FTISMC admittance control scheme.

collaborative robots are greatly improved, and human partners could be merged with the high performance of robots to complete much more complicated tasks together.

2. Compared to conventional admittance control,[2] the proposed approach integrates an admittance with fixed-time ISMC to guarantee robustness and fixed-time convergence, while compliant with external forces. Therefore, the proposed controller provides a faster transient response, lower tracking errors and better disturbance rejection capacity.
3. Compared to the existing FTISMC,[15–17] which uses the tracking errors and the velocity of the tracking errors to construct the integral sliding surface, the proposed controller develops a new nonsingular fixed-time integral sliding surface to avail of the full advantages of both ISMC and fixed-time techniques. The convergence time is independent of the initial conditions of the system and could be determined by the design parameters as a priori.

The article is organized as follows. The mathematical model describing the motion of a robot manipulator and the problem formulation is presented in Section 2. The proposed fixed-time ISMC scheme for admittance control is developed in Section 3. Simulation results demonstrating the effectiveness of the proposed controller are presented in Section 4. Finally, section 5 discusses the conclusions and directions for future works.

2 | PROBLEM FORMULATION AND PRELIMINARIES

2.1 | Problem formulation

We consider a robot manipulator whose joint space dynamics equation can be written in the form:

$$M(q)\ddot{q} + C(q,\dot{q})\dot{q} + G(q) + F(q) = \tau_c + \tau_e, \tag{1}$$

where q, $\dot{q}$, $\ddot{q}$ are the joint positions, velocities and accelerations of the robot manipulator, respectively. $q = \left[q_1, q_2, \ldots, q_N\right]^T$ and N is the number of joints. $M(q)$ is the $N \times N$ mass matrix, $C(q,\dot{q})$ is the $N \times N$ Coriolis and centrifugal forces matrix, $G(q)$ is the $N \times 1$ gravity vector, and $F(q)$ is the $N \times 1$ vector of frictional forces. τ_c denotes the control torque acting at the joints, and τ_e is the external torque from the interaction with the human partner. $F(q)$ and τ_e together form the time-varying lumped uncertainties of the system. Figure 2 above shows the structure of a classical two-link robot manipulator interacting physically with a human.

The task trajectory of robot is usually formulated in the Cartesian space. Therefore, we transfer the joint space dynamics of the robot manipulator (1) into Cartesian space:

$$M_x\ddot{x} + C_x\dot{x} + G_x + F_x = f_c + f_e, \tag{2}$$

where $x = [x_1, x_2, \ldots, x_R]$ represents the position of the end-effector in Cartesian space. To simplify the problem, we assume the robot is nonredundant ($R = N$). M_x, C_x, G_x, and F_x are coefficient matrices in Cartesian space, f_c is the control force, and f_e is the external force. The joint space velocities and Cartesian space velocities are related as:

$$\dot{x} = J(q)\dot{q}, \tag{3}$$

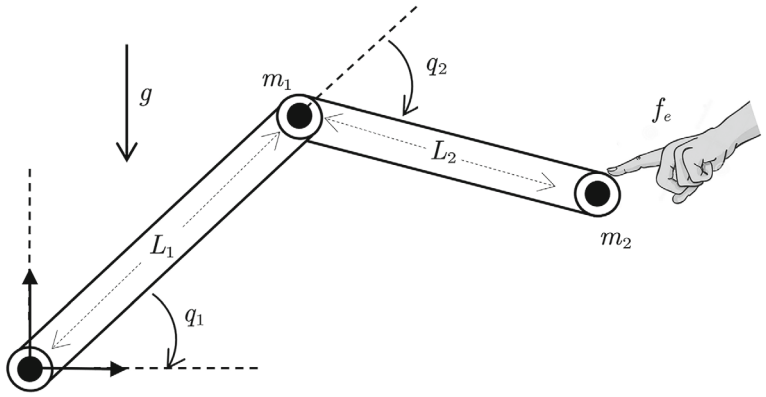

FIGURE 2 Two-link robot manipulator.

where $J(q)$ is the Jacobian of the robot manipulator. According to (3) and (1), the coefficient matrices in (2) can be written as:

$$\begin{aligned} M_x &= J^{-T}(q)M(q)J^{-1}(q), \\ C_x &= J^{-T}(q)\big(C(q,\dot{q}) - M(q)J^{-1}(q)\dot{J}(q)\big)J^{-1}(q), \\ G_x &= J^{-T}(q)G(q),\ F_x = J^{-T}(q)F(q), \\ f_c &= J^{-T}(q)\tau_c,\ \ f_e = J^{-T}(q)\tau_e. \end{aligned}$$

Letting $\eta_1 = x$ and $\eta_2 = \dot{x}$, the Cartesian space dynamics of the robot can be represented as:

$$\begin{cases} \dot{\eta}_1 = \eta_2, \\ \dot{\eta}_2 = M_x^{-1}(-C_x\dot{x} - G_x - F_x + f_e + f_c). \end{cases} \tag{4}$$

For ease of control design, let $\Xi = M_x^{-1}$, $\Gamma(x,\dot{x}) = M_x^{-1}(-C_x - G_x)$, $\Psi(x,\dot{x},t) = M_x^{-1}(-F_x + f_e)$, and $u = f_c$, such that the Cartesian space model can be further written as:

$$\begin{cases} \dot{\eta}_1 = \eta_2, \\ \dot{\eta}_2 = \Xi u + \Gamma(x,\dot{x}) + \Psi(x,\dot{x},t). \end{cases} \tag{5}$$

Assumption 1. There exists a positive constants ρ, such that the unknown lumped uncertainties term $\Psi(x,\dot{x},t)$ is bounded by:

$$\|\Psi(x,\dot{x},t)\| = \left\|M_x^{-1}(-F_x + f_e)\right\| \le \rho, \tag{6}$$

where ρ is a positive constant. The lumped uncertainties term $\Psi(x,\dot{x},t)$ is usually called unmatched uncertainties of the system and is upper bounded in Euclidean norm by a known constant ρ.

Remark 1. The above assumption is widely utilized in the design of ISMC controller,[23–25] which is usually practically satisfied because $\Psi(x,\dot{x},t)$ represents modelling uncertainties and external disturbances which could not be infinity. For very large disturbances, we expect that due to the high robustness of the closed-loop system, the effects could be mitigated gradually. If the $\Psi(x,\dot{x},t)$ is too large to satisfy Assumption 1, the problem tends to be too challenging and has beyond the scope of this article.

The control objective of this article is to develop a fixed-time integral sliding mode control scheme to make the Cartesian position x track a certain trajectory x_r which is generated from admittance control, aiming to obtain an overall compliant and stable behaviour of a robotic manipulator physically interacting with human partners. Therefore, the robot manipulator can perform human-friendly behaviors with higher tracking performance. Furthermore, we require that the tracking error converges within an arbitrarily small interval of time, regardless of the initial conditions.

2.2 | Preliminaries

Consider a time-varying differential equation:

$$\dot{x} = f(x, t), \tag{7}$$

where $x \in R^n$, and $f : R^n \to R^n$ is a continuous nonlinear function. Assume that the origin of (7) is the stable equilibrium point and $f(0) = 0$.

Definition 1 (9). The system (7) is finite time stable if the origin is Lyapunov stable and any solution $x(t)$ starting from x_0 satisfies $\lim_{t \to T(x_0)} x(t) \to 0$ and $x(t) = 0, \forall t > T(x_0)$, where $T(x_0)$ represents the settling time of the system.

Definition 2 (9). The system (7) is fixed-time stable if it is globally finite-time stable and its settling time $T(x_0)$ satisfies $T(x_0) < T_{\max}$, where $T_{\max}$ is a positive number.

Lemma 1 (14). *The following inequality holds for any real number that satisfies* $x_1, x_2, \ldots, x_n > 0$ *and* $0 < k < 1$:

$$\sum_{i=1}^{n} x_i^{k+1} \geq \left(\sum_{i=1}^{n} x_i^2 \right)^{\frac{k+1}{2}}. \tag{8}$$

Lemma 2 (14). *The following inequality holds for any real number that satisfies* $x_1, x_2, \ldots, x_n > 0$ *and* $k > 1$:

$$\sum_{i=1}^{n} x_i^k \geq n^{1-k} \left(\sum_{i=1}^{n} x_i \right)^k. \tag{9}$$

Lemma 3 (14). *Consider a scalar differential system below*:

$$\dot{y} = \lambda_1 [y]^\alpha + \lambda_2 [y]^\beta, \; y(0) = y_0, \tag{10}$$

where $\lambda_1, \lambda_2, \alpha, \beta$ *are all positive real numbers satisfying* $\lambda_1 > 0, \lambda_2 > 0, 0 < \alpha < 1$ *and* $\beta > 1$. $[y]^\alpha = |y|^\alpha sign(y)$. *Then the system (10) is fixed-time stable and the convergence time* T *is independent of the initial states of the system and bounded by*:

$$T < T_{\max}(\lambda_1, \lambda_2, \alpha, \beta) := \frac{1}{\lambda_1(1-\alpha)} + \frac{1}{\lambda_2(\beta - 1)}. \tag{11}$$

3 | CONTROL DESIGN AND STABILITY ANALYSIS

3.1 | Admittance trajectory shaping

To achieve so-called compliance of robot manipulator, the contact point between robot and human can be modeled as a mass-spring-damper system, which is shown in Figure 3. The objective of modeling the system with virtual mass, spring and damper is to make sure the interaction forces are elastic and never vibrate at the contact point.

Let $\xi_i = x_{r_i} - x_{d_i}, i = 1, 2, \ldots, N$, where the x_{r_i} is the reference trajectory generated from admittance control and the x_{d_i} is the initial desired trajectory of the robot manipulator. The dynamics for a robot manipulator rendering an impedance can be written as:

$$k_{m_i} \ddot{\xi}_i + k_{b_i} \dot{\xi}_i + k_{k_i} \xi_i = f_{e_i}, \tag{12}$$

where k_{m_i}, k_{b_i}, and k_{k_i} are mass, spring and damping coefficient. f_e is the external human force. By integrating the impedance equation (12), we obtain x_{r_i} which will be tracked by the controller.

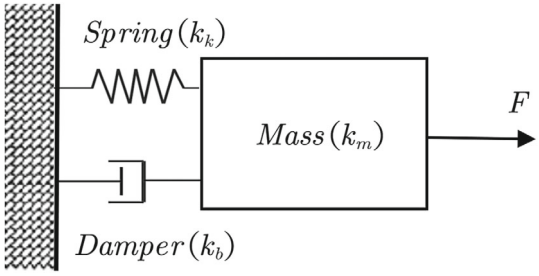

FIGURE 3 The mass-spring-damper system.

3.2 | Design of fixed-time ISMC

Let the tracking error be written as:

$$e = x - x_r, \tag{13}$$

where x_r is the reference trajectory generated from the admittance control, and x is the real trajectory of the robot. The derivative of tracking error e is $\dot{e} = \dot{x} - \dot{x}_r$. To obtain the fixed-time convergence of system, we reconstruct the tracking error based on Lemma 3 as:

$$s = \dot{e} + k_1[e]^{\alpha} + k_2[e]^{\beta}, \tag{14}$$

where k_1, k_2, α, β are all positive constants satisfying $k_1, k_2 > 0$, $0 < \alpha < 1$, and $\beta > 1$. When the s converges to zero, (14) can be rewritten as:

$$\dot{e} = -k_1[e]^{\alpha} - k_2[e]^{\beta}. \tag{15}$$

According to Lemma 3, the convergence time of s is bounded by:

$$T_{s1} \leq \frac{1}{k_1(1-\alpha)} + \frac{1}{k_2(\beta-1)}. \tag{16}$$

Differentiating (14) with respect to time and using (5), we have:

$$\dot{s} = \ddot{x} - \ddot{x}_r + k_1\alpha[e]^{\alpha-1}\dot{e} + k_2\beta[e]^{\beta-1}\dot{e} = \Xi u + \Gamma(x,\dot{x}) + \Psi(x,\dot{x},t) - \ddot{x}_r + k_1\alpha[e]^{\alpha-1}\dot{e} + k_2\beta[e]^{\beta-1}\dot{e}. \tag{17}$$

Based on (14) and (17), the integral sliding surface is selected as:

$$\sigma_1(t) = s(t) - s(0) - \int_0^t \left(\Xi u_0 + \Gamma(x,\dot{x}) - \ddot{x}_r + k_1\alpha[e]^{\alpha-1}\dot{e} + k_2\beta[e]^{\beta-1}\dot{e}\right)dt, \tag{18}$$

where term $s(0)$ represents the value of the sliding surface when $t = 0$. u_0 is the output of the nominal controller, which is designed for the nondisturbance system by another method and will be presented in the Section 3.4.

Assumption 2 (23). For the nominal system which is the system (5) without the lumped uncertainties term:

$$\begin{cases} \dot{\eta}_1 = \eta_2, \\ \dot{\eta}_2 = \Xi u + \Gamma(x,\dot{x}). \end{cases} \tag{19}$$

The system (19) is globally asymptotically stabilizable via a nominal control u_0.

Remark 2. After we design a controller which drives the integral sliding surface $\sigma_1(t)$ to the zero, three terms (i.e., $s(t)$, $s(0)$ and integral term $\int_0^t \left(\Xi u_0 + \Gamma(x,\dot{x}) - \ddot{x}_r + k_1\alpha[e]^{\alpha-1}\dot{e} + k_2\beta[e]^{\beta-1}\dot{e}\right)dt$) in (18) will all be forced to

converge to zero simultaneously. When $s(t) = 0$, we have (15) and (16) hold. Therefore, $s(t)$ will also converge to zero within a fixed time. The term $-s(0)$ provides a nice property, $\sigma_1(0) = 0$, which eliminates the reaching phase of traditional SMC, and therefore enforce the sliding phase throughout the entire closed-loop system response to ensure the robustness. In the integral term, nominal controller u_0 is assumed that it has already ensure the asymptotic stability of the system, and the proposed controller is designed as an "add-on" to the u_0 to achieve better tracking performance. Additionally, the integral term provides one more degree of freedom for sliding surface design. We add $k_1\alpha[e]^{\alpha-1}\dot{e} + k_2\beta[e]^{\beta-1}\dot{e}$ to achieve fixed-time convergence of proposed system. Details will be given later in the this section.

The derivative of the integral sliding surface can be further written as:

$$\begin{aligned}\dot{\sigma_1}(t) = &\left(\Xi u + \Gamma(x,\dot{x}) + \Psi(x,\dot{x},t) - \ddot{x}_r + k_1\alpha[e]^{\alpha-1}\dot{e} + k_2\beta[e]^{\beta-1}\dot{e}\right)\\ &- \left(\Xi u_0 + \Gamma(x,\dot{x}) - \ddot{x}_r + k_1\alpha[e]^{\alpha-1}\dot{e} + k_2\beta[e]^{\beta-1}\dot{e}\right),\end{aligned} \tag{20}$$

Therefore, we have:

$$\dot{\sigma_1}(t) = \Xi(u - u_0) + \Psi(x,\dot{x},t).$$

Letting $u = u_0 + u_{s1}$, where u_{s1} is designed to compensate for disturbances based on u_0, we obtain:

$$\dot{\sigma_1}(t) = \Xi u_{s1} + \Psi(x,\dot{x},t). \tag{21}$$

In (21), the proposed compensating controller u_{s1} is designed as:

$$u_{s1} = \Xi^{-1}\left(-(\rho+\varepsilon)\,sign\,(\sigma_1) - k_3[\sigma_1]^p - k_4[\sigma_1]^q\right), \tag{22}$$

where the $k_3, k_4 > 0$, $0 < p < 1$ and $q > 1$. Inserting the compensating controller u_{s1} into (21), yields:

$$\dot{\sigma_1}(t) = \Psi(x,\dot{x},t) - (\rho+\varepsilon)\,sign\,(\sigma_1) - k_3[\sigma_1]^p - k_4[\sigma_1]^q, \tag{23}$$

where ε is a small positive constant. For $i = 1, 2, \ldots, N$, we have:

$$\dot{\sigma_{1_i}}(t) = \Psi_i(x,\dot{x},t) - (\rho+\varepsilon)\,sign\left(\sigma_{1_i}\right) - k_3\left[\sigma_{1_i}\right]^p - k_4\left[\sigma_{1_i}\right]^q. \tag{24}$$

Consider a Lyapunov function candidate:

$$V_1 = \frac{1}{2}\sum_{i=1}^{N}\sigma_{1_i}^2. \tag{25}$$

Differentiating the Lyapunov function (25), we have:

$$\begin{aligned}\dot{V}_1 &= \sum_{i=1}^{N}\sigma_{1_i}\dot{\sigma_{1_i}}\\ &= \sum_{i=1}^{N}\sigma_{1_i}\left(\Psi_i(x,\dot{x},t) - (\rho+\varepsilon)sign\left(\sigma_{1_i}\right) - k_3\left[\sigma_{1_i}\right]^p - k_4\left[\sigma_{1_i}\right]^q\right)\\ &= \sum_{i=1}^{N}\left(\sigma_{1_i}\Psi_i(x,\dot{x},t) - (\rho+\varepsilon)\left|\sigma_{1_i}\right| - k_3\left|\sigma_{1_i}\right|^{p+1} - k_4\left|\sigma_{1_i}\right|^{q+1}\right).\end{aligned} \tag{26}$$

By using Assumption 1, we have:

$$\dot{V}_1 \le \sum_{i=1}^{N}\left(-k_3\left|\sigma_{1_i}\right|^{p+1} - k_4\left|\sigma_{1_i}\right|^{q+1}\right). \tag{27}$$

By using Lemma 1 and Lemma 2, we have:

$$\begin{aligned}\dot{V}_1 &\leq -k_3\sum_{i=1}^{N}|\sigma_{1_i}|^{p+1} - k_4\sum_{i=1}^{N}|\sigma_{1_i}|^{q+1}\\ &\leq -k_3\sum_{i=1}^{N}\left(|\sigma_{1_i}|^2\right)^{\frac{p+1}{2}} - k_4\sum_{i=1}^{N}\left(|\sigma_{1_i}|^2\right)^{\frac{q+1}{2}}\\ &\leq -k_3\left(\sum_{i=1}^{N}|\sigma_{1_i}|^2\right)^{\frac{p+1}{2}} - k_4N^{\frac{1-q}{2}}\left(\sum_{i=1}^{N}|\sigma_{1_i}|^2\right)^{\frac{q+1}{2}}\\ &= -k_3 2^{\frac{p+1}{2}}(V_1)^{\frac{p+1}{2}} - k_4 2^{\frac{q+1}{2}}N^{\frac{1-q}{2}}(V_1)^{\frac{q+1}{2}}.\end{aligned} \tag{28}$$

Based on the Lemma 3, the above system is fixed-time stable and the convergence time is upper bounded as:

$$T_{r1} \leq \frac{1}{2^{\frac{p+1}{2}}k_3\left(1-\frac{p+1}{2}\right)} + \frac{1}{2^{\frac{q+1}{2}}k_4N^{\frac{1-q}{2}}\left(\frac{q+1}{2}-1\right)}. \tag{29}$$

Theorem 1. *The system (5) with controller u_{s1} is fixed-time stable and the settling time is bounded by*:

$$T \leq T_{s1} + T_{r1} + T_n, \tag{30}$$

where T_{s1} and T_{r1} represent the convergence time of the sliding variable s *and the system (5) with u_{s1} as the controller, respectively. T_n represents the convergence time of the system (5) with u_0 as the nominal controller, which will be determined in Section 3.4.*

Proof. It is clear that the convergence time of the entire system is smaller than the sum of the convergence times of each component (i.e., the convergence time of the sliding surface, compensating controller and nominal controller). This completes the proof. ∎

Remark 3. The value for ρ of the controller in (22) was selected based on Assumption 1. In practice, we can use experiments to determine the bounded value of the uncertainty ρ. Another method which can be applied to approximate the value of the parameter of ρ is to use an adaptive technique. For example, we can use an adaptive second-order super-twisting method[22] to estimate the adaptive gain and eliminate the chattering at the same time.

Remark 4. The use of the 'sign' function in the controller (22) will generate a chattering. To eliminate the chattering, a boundary layer method or second-order super-twisting method can be employed.[22]

3.3 | Nonsingular problem

In (17), when $e = 0$ and $\dot{e} \neq 0$ the term $k_1\alpha[e]^{\alpha-1}\dot{e}$ results in a singular problem. To avoid the singularity, we reconstruct the error in an alternative form:

$$s = e + \frac{1}{k_5^m}\left[\dot{e} + k_6[e]^n\right]^{\frac{1}{m}}, \tag{31}$$

where $k_5, k_6,$ m, n are all positive constants satisfying $k_5, k_6 > 0, 0 < m < 1$, and $n > 1$. When the sliding surface variable converges to zero, (31) is equal to (14). Therefore, we can still ensure the fixed-time convergence of s without the singular problem. According to the Lemma 3, the convergence time of s is bounded by:

$$T_{s2} \leq \frac{1}{k_5(1-m)} + \frac{1}{k_6(n-1)}. \tag{32}$$

Differentiating (31) with respect to time, we have:

$$\dot{s} = \dot{e} + \frac{1}{mk_5^m}|\dot{e} + k_6[e]^n|^{\frac{1}{m}-1}\left(\ddot{e} + k_6n[e]^{n-1}\dot{e}\right). \tag{33}$$

The integral sliding surface is selected as:

$$\sigma_2(t) = s(t) - s(0) - \int_0^t \left(\dot{e} + \frac{1}{mk_5^m} |\dot{e} + k_6[e]^n|^{\frac{1}{m}-1} \left(\ddot{e} + k_6 n[e]^{n-1} \right) \dot{e} \right) dt. \tag{34}$$

According to the (5), we have:

$$\ddot{e} = \ddot{x} - \ddot{x}_r = \Xi u + \Gamma(x, \dot{x}) - \ddot{x}_r. \tag{35}$$

Inserting (35) into (34) and letting:

$$\begin{aligned} T_1(e, \dot{e}) &= \frac{1}{mk_5^m} |\dot{e} + k_6[e]^n|^{\frac{1}{m}-1}, \\ T_2(e) &= k_6 n[e]^{n-1} \dot{e}. \end{aligned} \tag{36}$$

The derivative of integral sliding surface can be written as:

$$\dot{\sigma_2}(t) = (\dot{e} + T_1(e, \dot{e})(\Xi u + \Gamma(x, \dot{x}) + \Psi(x, \dot{x}, t) - \ddot{x}_r + T_2(e))) - (\dot{e} + T_1(e, \dot{e})(\Xi u_0 + \Gamma(x, \dot{x}) - \ddot{x}_r + T_2(e))). \tag{37}$$

Setting $u = u_0 + u_{s2}$, we have:

$$\dot{\sigma_2}(t) = T_1(e, \dot{e})(\Xi u_{s2} + \Psi(x, \dot{x}, t)). \tag{38}$$

Again, the controller u_{s2} can be designed as:

$$u_{s2} = \Xi^{-1} \left(-(\rho + \varepsilon) \, sign(\sigma_2) - k_5[\sigma_2]^m - k_6[\sigma_2]^n \right). \tag{39}$$

Inserting the compensating controller into (38), we have:

$$\dot{\sigma_2}(t) = T_1(e, \dot{e}) \left(\Psi(x, \dot{x}, t) - (\rho + \varepsilon) \, sign(\sigma_2) - k_5[\sigma_2]^m - k_6[\sigma_2]^n \right). \tag{40}$$

Considering a Lyapunov function candidate:

$$V_2 = \frac{1}{2} \sum_{i=1}^{N} \sigma_{2_i}^2. \tag{41}$$

Differentiating the Lyapunov function (25), we have:

$$\begin{aligned} \dot{V}_2 &= \sum_{i=1}^{N} \sigma_{2_i} \dot{\sigma_{2_i}} \\ &= \sum_{i=1}^{N} \sigma_{2_i} T_1(e, \dot{e}) \left(\Psi_i(x, \dot{x}, t) - (\rho + \varepsilon) sign\left(\sigma_{2_i}\right) - k_5 \left[\sigma_{2_i}\right]^m - k_6 \left[\sigma_{2_i}\right]^n \right) \\ &= T_1(e, \dot{e}) \sum_{i=1}^{N} \left(\sigma_{2_i} \Psi_i(x, \dot{x}, t) - (\rho + \varepsilon) |\sigma_{2_i}| - k_5 |\sigma_{2_i}|^{m+1} - k_6 |\sigma_{2_i}|^{n+1} \right) \\ &\le T_1(e, \dot{e}) \sum_{i=1}^{N} \left(-k_5 |\sigma_{2_i}|^{m+1} - k_6 |\sigma_{2_i}|^{n+1} \right) \\ &\le T_1(e, \dot{e}) \left(-k_5 2^{\frac{m+1}{2}} (V_2)^{\frac{m+1}{2}} - k_6 2^{\frac{n+1}{2}} N^{\frac{1-n}{2}} (V_2)^{\frac{n+1}{2}} \right). \end{aligned} \tag{42}$$

Theorem 2. *The system (5) with controller u_{s2} is fixed-time stable and its settling time is bounded by*:

$$T \le T_{s2} + T_{r2} + T_n + \varepsilon(\gamma), \tag{43}$$

where T_{s2} and T_{r2} represent the convergence time of sliding variable s *and the system (5) with u_{s2} as the controller, respectively. T_n represent the convergence time of the system (5) with u_0 as the nominal controller, and $\varepsilon(\gamma)$ denotes a small time margin related to the boundary width $\gamma = \left(mk_5^m\right)^{\frac{m}{1-m}}$.*

Proof. From (40), we can see the fixed-time stability depends both on the term $-k_5 2^{\frac{m+1}{2}}(V_2)^{\frac{m+1}{2}} - k_6 2^{\frac{n+1}{2}} N^{\frac{1-n}{2}}(V_2)^{\frac{n+1}{2}}$ and the term $T_1(e,\dot{e})$. Inspired by the work of Li and Cai,[26] for the case of $\kappa = \dot{e} + k_6[e]^n \neq 0$, we divide the state space into two different areas $\Omega_1 = \{(e,\dot{e})|T(e,\dot{e}) \geq 1\}$ and $\Omega_2 = \{(e,\dot{e})|T(e,\dot{e}) < 1\}$. ∎

1. When the system states are in the area of Ω_1, we have:

$$|\kappa| \geq \gamma = \left(mk_5^m\right)^{\frac{m}{1-m}} \tag{44}$$

and

$$\dot{V}_2 \leq -k_5 2^{\frac{m+1}{2}}(V_2)^{\frac{m+1}{2}} - k_6 2^{\frac{n+1}{2}} N^{\frac{1-n}{2}}(V_2)^{\frac{n+1}{2}}, \tag{45}$$

$V_2 = 0$ implies the sliding surface $\sigma_2 = 0$. Therefore, according to the Lemma 3, the system states will reach the sliding surface $\sigma_2 = 0$ or enter the Ω_2 within a fixed time, which is bounded by:

$$T_{r2} \leq \frac{1}{2^{\frac{m+1}{2}} k_5\left(1 - \frac{m+1}{2}\right)} + \frac{1}{2^{\frac{n+1}{2}} k_6 N^{\frac{1-n}{2}}\left(\frac{n+1}{2} - 1\right)}. \tag{46}$$

2. When the system states are in the area of Ω_2, it is clear that $0 < T(e,\dot{e}) < 1$ when $\kappa \neq 0$. According to (42), the sliding surface $\sigma_2 = 0$ is still an attractor. In addition, for the special case of $\dot{e} + k_6[e]^n = 0$, according to the (34) and (40), both σ_2 and $\dot{\sigma_2}$ are equal to 0. The system is on the equilibrium point. Therefore, for a given γ, there exists a positive constant $\varepsilon(\gamma)$ such that the sliding surface σ_2 can be reached from anywhere in the phase plane within fixed time within a fixed time $t_r < T_{r2} + \varepsilon(\gamma)$.[26] Therefore, the total setting time T is bounded as (43). This completes the proof.

Remark 5. Compared to the design of the integral sliding surfaces of the existing FTISMC,[15–17] the proposed controller uses the sliding surface in (34), which takes the dynamics of the system account in the design of the integral sliding surface. This approach provides two advantages: (1) it allows us to design the nominal controller u_0 and the reaching controller u_s separately. This facilitates the design procedure and preserves the advantages of both the nominal controller and ISMC.

3.4 | Design of the nominal controller

The nominal controller is designed to stabilize the system neglecting the lumped uncertainties. To stabilize the whole system within a fixed time, we choose fixed-time backstepping control[27] as the nominal controller. The dynamics of the robot manipulator without lumped uncertainties can be written as:

$$\begin{cases} \dot{\eta}_1 = \eta_2, \\ \dot{\eta}_2 = \Xi u + \Gamma(x,\dot{x}). \end{cases} \tag{47}$$

Letting $s_1 = \eta_1 - x_r$, then, $\dot{s}_1 = \eta_2 - \dot{x}_r$, and we can design the stabilizing function as:

$$\alpha_s = -\left(\lambda_1 s_1 + \lambda_2 s_1^{\alpha} + \lambda_3 s_1^{\beta}\right) + \dot{x}_r, \tag{48}$$

where λ_1, λ_2, λ_3, α, β are all positive constants satisfying $0 < \alpha < 1$ and $\beta > 1$. Thus, $\dot{s}_1$ can be written as:

$$\dot{s}_1 = -\left(\lambda_1 s_1 + \lambda_2 s_1^{\alpha} + \lambda_3 s_1^{\beta}\right). \tag{49}$$

Selecting the Lyapunov function candidate as:

$$V_3 = \frac{1}{2} s_1^T s_1. \tag{50}$$

The derivative of the Lyapunov function V_3 is:

$$\begin{aligned}
\dot{V}_3 &= s_1^T \dot{s}_1 \\
&= -s_1^T \left(\lambda_1 s_1 + \lambda_2 s_1^{\alpha} + \lambda_3 s_1^{\beta} \right) \\
&= -\lambda_1 s_1^T s_1 - \lambda_2 \left(s_1^T s_1 \right)^{\frac{\alpha+1}{2}} - \lambda_3 \left(s_1^T s_1 \right)^{\frac{\beta+1}{2}} \\
&\leq -\lambda_2 \left(s_1^T s_1 \right)^{\frac{\alpha+1}{2}} - \lambda_3 \left(s_1^T s_1 \right)^{\frac{\beta+1}{2}} \\
&\leq -2^{\frac{\alpha+1}{2}} \lambda_2 \left(\frac{1}{2} s_1^T s_1 \right)^{\frac{\alpha+1}{2}} - 2^{\frac{\beta+1}{2}} \lambda_3 \left(\frac{1}{2} s_1^T s_1 \right)^{\frac{\beta+1}{2}} \\
&= -2^{\frac{\alpha+1}{2}} \lambda_2 (V_3)^{\frac{\alpha+1}{2}} - 2^{\frac{\beta+1}{2}} \lambda_3 (V_3)^{\frac{\beta+1}{2}}.
\end{aligned} \tag{51}$$

Letting $s_2 = \eta_2 - \alpha_s$, we have:

$$\dot{s}_2 = \dot{\eta}_2 - \dot{\alpha}_s = \Xi u_0 - \Gamma(x, \dot{x}) - \dot{\alpha}_s. \tag{52}$$

Selecting the Lyapunov function candidate as:

$$V_4 = \frac{1}{2} s_2^T s_2. \tag{53}$$

To obtain the property of fixed-time convergence, we design the nominal controller as:

$$u_0 = \Xi^{-1} \left(-\Gamma(x, \dot{x}) + \dot{\alpha}_s - \lambda_1 s_2 - \lambda_2 s_2^{\alpha} - \lambda_3 s_2^{\beta} \right). \tag{54}$$

Inserting (54) into (52), we have:

$$\dot{s}_2 = -\lambda_1 s_2 - \lambda_2 s_2^{\alpha} - \lambda_3 s_2^{\beta}. \tag{55}$$

The derivative of the Lyapunov function V_2 is:

$$\begin{aligned}
\dot{V}_4 &= s_2^T \dot{s}_2 \\
&= s_2^T \left(-\lambda_1 s_2 - \lambda_2 s_2^{\alpha} - \lambda_3 s_2^{\beta} \right) \\
&\leq -2^{\frac{\alpha+1}{2}} \lambda_2 (V_4)^{\frac{\alpha+1}{2}} - 2^{\frac{\beta+1}{2}} \lambda_3 (V_4)^{\frac{\beta+1}{2}}.
\end{aligned} \tag{56}$$

Choosing the Lyapunov function candidate of system as:

$$V_n = V_3 + V_4. \tag{57}$$

The derivative of Lyapunov function V is:

$$\begin{aligned}
\dot{V}_n &\leq -2^{\frac{\alpha+1}{2}} \lambda_2 (V_3)^{\frac{\alpha+1}{2}} - 2^{\frac{\beta+1}{2}} \lambda_3 (V_3)^{\frac{\beta+1}{2}} - 2^{\frac{\alpha+1}{2}} \lambda_2 (V_4)^{\frac{\alpha+1}{2}} - 2^{\frac{\beta+1}{2}} \lambda_3 (V_4)^{\frac{\beta+1}{2}} \\
&\leq -2^{\frac{\alpha+1}{2}} \lambda_2 (V_n)^{\frac{\alpha+1}{2}} - 2^{\frac{\beta+1}{2}} \lambda_3 (V_n)^{\frac{\beta+1}{2}}.
\end{aligned} \tag{58}$$

According to the Lemma 3, when applying the proposed nominal controller u_0, the system without lumped uncertainties is fixed-time stable and the convergence time is bounded as:

$$T_n \leq \frac{2}{\lambda_2 2^{\frac{\alpha+1}{2}} (1-\alpha)} + \frac{2}{\lambda_3 2^{\frac{\beta+1}{2}} (\beta-1)}. \tag{59}$$

Remark 6. It is noted that the nominal controller can be designed using other controllers, for example, PID, CTC or Backstepping controller. However, in this article, we use the fixed-time backstepping controller to achieve global fixed-time convergence for the system.

4 | SIMULATION AND RESULTS

In the simulation, we consider a two-link robot in the horizontal plane.[28] The dynamics of the robot are described as:

$$\begin{aligned}\tau_1 &= m_2 l_2^2\left(\ddot{q}_1+\ddot{q}_2\right)+m_2 l_1 l_2 c_2\left(2\ddot{q}_1+\ddot{q}_2\right)+(m_1+m_2) l_1^2 \ddot{q}_1-m_2 l_1 l_2 s_2 \dot{q}_2^2-2 m_2 l_1 l_2 s_2 \dot{q}_1 \dot{q}_2+m_2 l_2 g c_{12}+(m_1+m_2) l_1 g c_1\\ \tau_2 &= m_2 l_1 l_2 c_2 \ddot{q}_1+m_2 l_1 l_2 s_2 \dot{q}_1^2+m_2 l_2 g c_{12}+m_2 l_2^2\left(\ddot{q}_1+\ddot{q}_2\right),\end{aligned} \tag{60}$$

where $c_i = \cos(q_i)$, $c_{ij} = \cos\left(q_i + q_j\right)$, $s_i = \sin(q_i)$, and $s_{ij} = \sin\left(q_i + q_j\right)$, $i, j = 1, 2$. The value of masses are $m_1 = 1.5$ kg, and $m_2 = 1.0$ kg. The length of the links are $l_1 = l_2 = 0.3$ m. Based on the (1), the mass matrix $M(q)$, Coriolis and centrifugal forces matrix $C(q, \dot{q})$ and the gravity matrix $G(q)$ are given as:

$$M(q) = \begin{bmatrix} m_2 l_2^2 + 2m_2 l_1 l_2 c_2 + (m_1+m_2) l_1^2 & m_2 l_2^2 + m_2 l_1 l_2 c_2 \\ m_2 l_2^2 + m_2 l_1 l_2 c_2 & m_2 l_2^2 \end{bmatrix}, \tag{61}$$

$$C(q, \dot{q}) = \begin{bmatrix} -2m_2 l_1 l_2 s_2 \dot{q}_2 & -m_2 l_1 l_2 s_2 \\ m_2 l_1 l_2 s_2 \dot{q}_1 & 0 \end{bmatrix}, \tag{62}$$

$$G(q) = \begin{bmatrix} m_2 l_2 g c_{12} + (m_1+m_2) l_1 g c_1 \\ m_2 l_2 g c_{12} \end{bmatrix}. \tag{63}$$

The bounded disturbance term is given as:

$$F(q) = \begin{bmatrix} 2c_1 s_2 + 5c_1^2 \\ -2c_1 s_2 - 5c_1^2 \end{bmatrix}. \tag{64}$$

The Jacobian of the robot manipulator is given as:

$$J(q) = \begin{bmatrix} -l_1 s_1 - l_2 s_{12} & -l_2 s_{12} \\ l_1 c_1 + l_2 c_{12} & l_2 c_{12} \end{bmatrix}. \tag{65}$$

Assume the desired trajectory[3] of the two joints is:

$$\begin{aligned} x_{d1}(t) &= 0.14\cos(0.5t), \\ x_{d2}(t) &= 0.14\sin(0.5t). \end{aligned} \tag{66}$$

The external human forces, as shown in Figure 4, are given by[3]:

$$fe_i(t)\begin{cases} 0 & t < 10 \text{ or } t \geq 21, \\ a_i(1-\cos \pi t) & 10 \leq t < 11, \\ 2a_i & 11 \leq t < 20, \\ a_i(1+\cos \pi t) & 20 \leq t < 21. \end{cases} \tag{67}$$

The external human forces are applied when $t = 10$ s and removed at $t = 21$ s. By applying admittance control, the reference trajectory of the two joints x_{r1} and x_{r2} can be derived by integrating equation (12) twice. Figure 5 shows both the desired trajectory and the reference trajectory. We can see the two trajectories are the same before the external forces are applied. When $t > 10$ s, the reference trajectory, which complies with the external human forces, is different from the

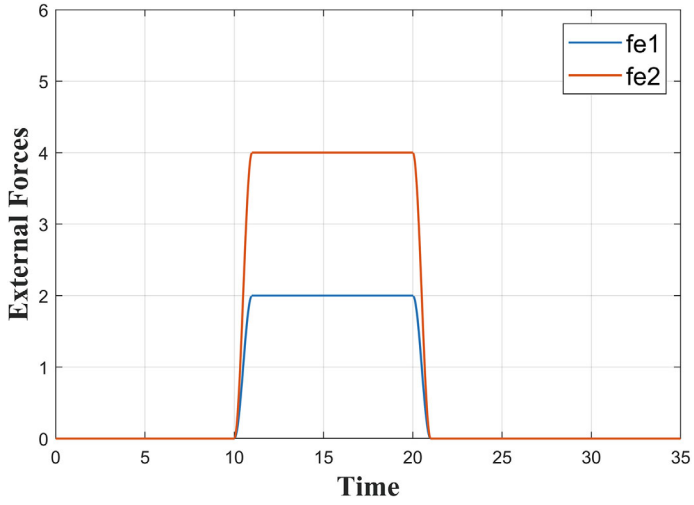

FIGURE 4 External human forces.

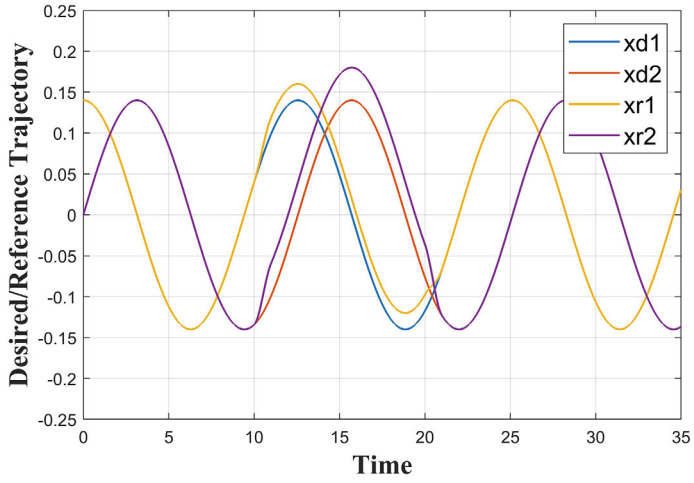

FIGURE 5 Desired/reference trajectory.

desired trajectory. When $t > 21$ s, the external human forces are removed from the contact point and the two trajectories coincide again.

To verify the effectiveness of the proposed controller, we compare it with PID, computed torque control (CTC), traditional ISMC with PID as the nominal controller (ISMC PID), traditional ISMC with CTC as the nominal controller (ISMC CTC), and traditional ISMC with BSP as the nominal controller (ISMC BSP). The PID is designed as $f_c = K_p e(t) + K_i \int e(t)dt + K_d \dot{e}(t)$. The CTC is designed as $f_c = M_x\left(\ddot{x}_r(t) + K_p e(t) + K_i \int e(t)dt + K_d \dot{e}(t)\right) + C_x \dot{x} + G_x$. Assume the initial position of the end-effector is $q(0) = [0.5236, 2.0944]^T$, and the initial value of the task variable is $x(0) = [0, 0]^T$. The design parameters of the admittance control are $k_{m_i} = 20$, $k_{b_i} = 20$ and $k_{k_i} = 100$, $i = 1, 2$. The parameters of PID and CTC are selected as $k_p = 300$, $k_d = 400$, $k_i = 10$. The parameters of BSP are selected as $\lambda_1 = 3$, $\lambda_2 = 20$, $\lambda_3 = 50$, $\alpha = \frac{5}{7}$, $\beta = \frac{5}{3}$. The design parameters of the proposed controller are $k_1 = k_3 = k_5 = 20$, $k_2 = k_4 = k_6 = 50$, $m = p = \frac{5}{7}$, $n = q = \frac{5}{3}$.

Remark 7. For the parameters of admittance control k_{m_i}, k_{b_i}, and k_{k_i}, we selected as that in the work of Tee et al.[3] The parameters k_p, k_d, k_i of PID, CTC, ISMC-PID and ISMC CTC are all same, which are selected based on a trial-and-error procedure and by experience. The parameters of fixed-time terms are selected by their corresponding equations of settling time (32) (46) (59). For example, The parameters of fixed-time ISMC including $k_1, k_2, k_3, k_4, k_5, k_6$. We can see that bigger $k_1, k_2, k_3, k_4, k_5, k_6$ lead to shorter settling time and smaller tracking error, however, also implies more control effort and greater chattering because the employment of

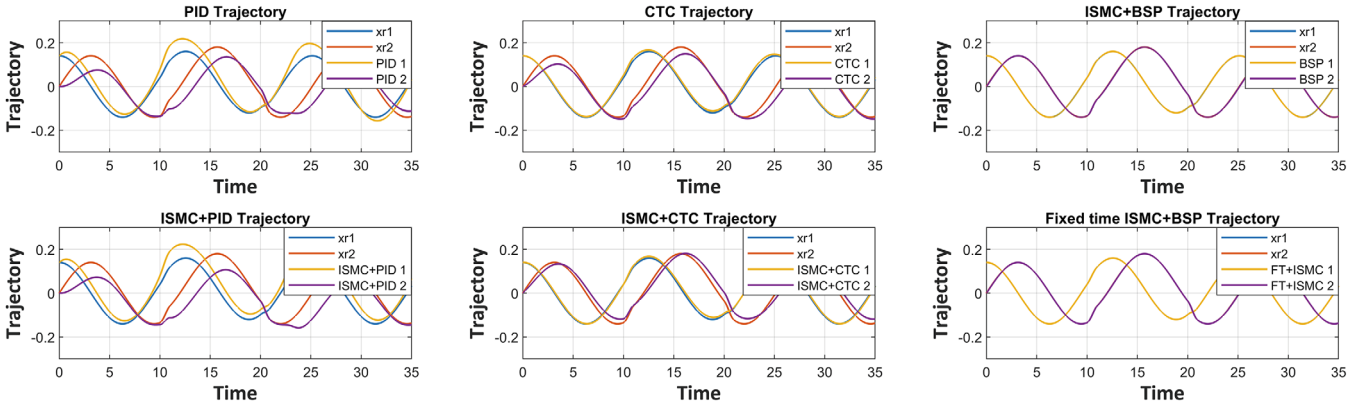

FIGURE 6 Trajectories obtained with the different controllers.

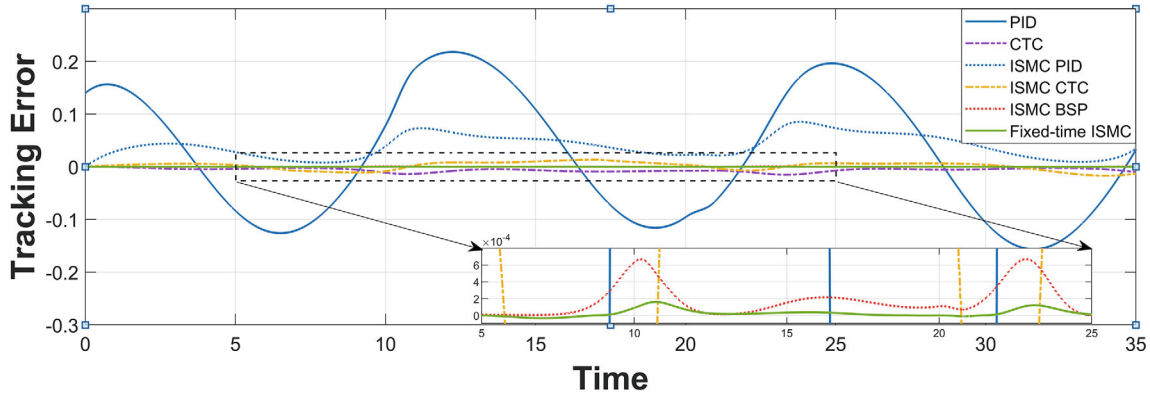

FIGURE 7 Tracking error for joint 1.

TABLE 1 The RMSE performance of each controller.

Joint	PID	CTC	ISMC+PID	ISMC+CTC	ISMC+BSP	FTISMC+BSP
1	0.1211	0.0070	0.0446	0.0064	2.0901×10^{-4}	5.7841×10^{-5}
2	0.0845	0.0314	0.0644	0.0220	0.0016	4.4889×10^{-4}

the 'sign' functions. Therefore, we could gradually decrease the preset values of these parameters until a good performance of the closed-loop system is obtained and the chattering problem is acceptable. This turning way is also applied to the parameters of the fixed-time BSP such as λ_2 and λ_3. The rest parameters are α, β, m, n, p, q, we can just select $0 < \alpha, m, p < 1$ and $\beta, n, q > 1$ as the requirements of the Lemma 3.

The trajectories of the benchmark controllers and the proposed fixed-time ISMC controller with BSP as the nominal controller are shown in Figure 6, and the corresponding root mean square error (RMSE) of tracking errors are reported in Table 1. We can see that the PID controller has the poorest tracking performance. The performance of CTC is a little better than PID. The performance of ISMCPID and ISMC CTC are better than pure PID and CTC, respectively, which means the tracking performance of the controller is improved by adding the integral sliding surface. The ISMC BSP and proposed fixed-time ISMC controller have the best tracking performance. They almost achieve perfect tracking of the reference trajectory, which makes it difficult to compare them in Figure 6. However, as can be seen in Figures 7 and 8, it is clear that the proposed controller has both the smallest tracking error and the shortest convergence time. Note that the proposed controller is global fixed-time convergent because both the integral sliding surface, reaching controller and the nominal controller can converge within a fixed time. In addition, from Figures 9 and 10, which show the control inputs of the two joints, it can be seen that the proposed solution provides the smoothest and most efficient control input.

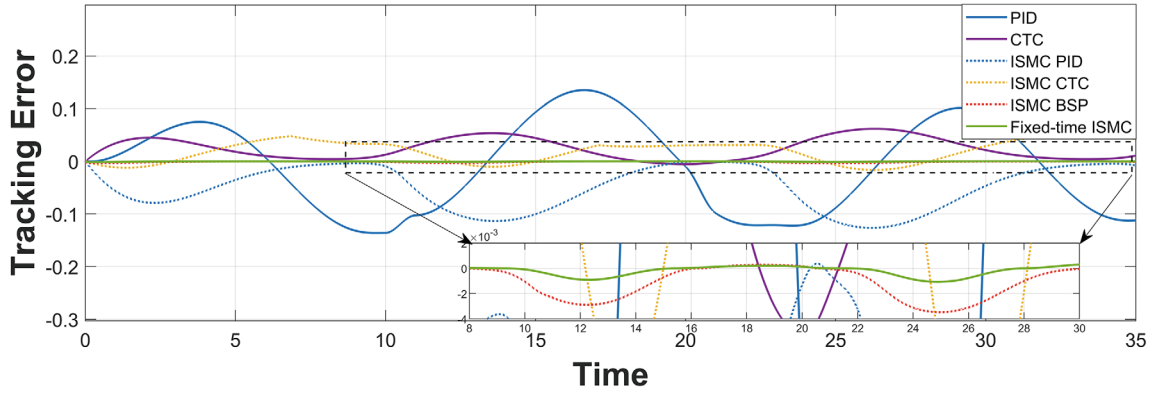

FIGURE 8 Tracking error for joint 2.

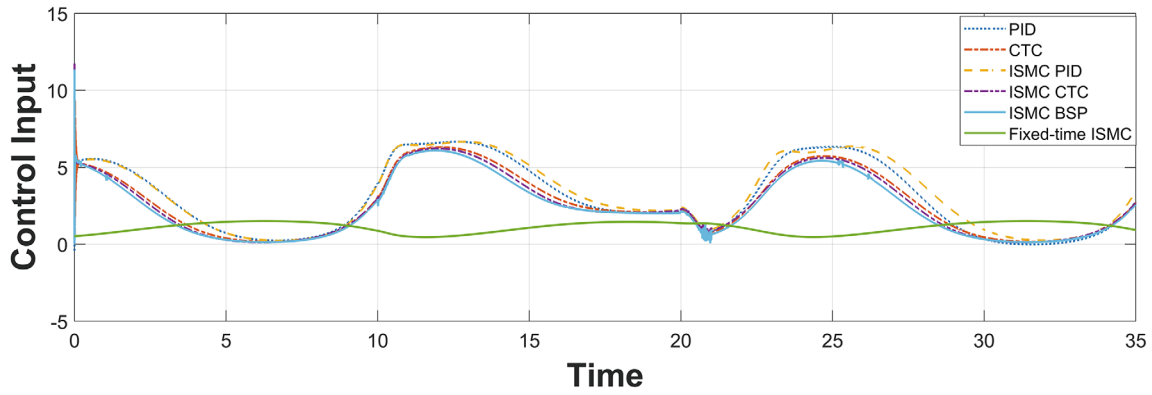

FIGURE 9 Control input for joint 1.

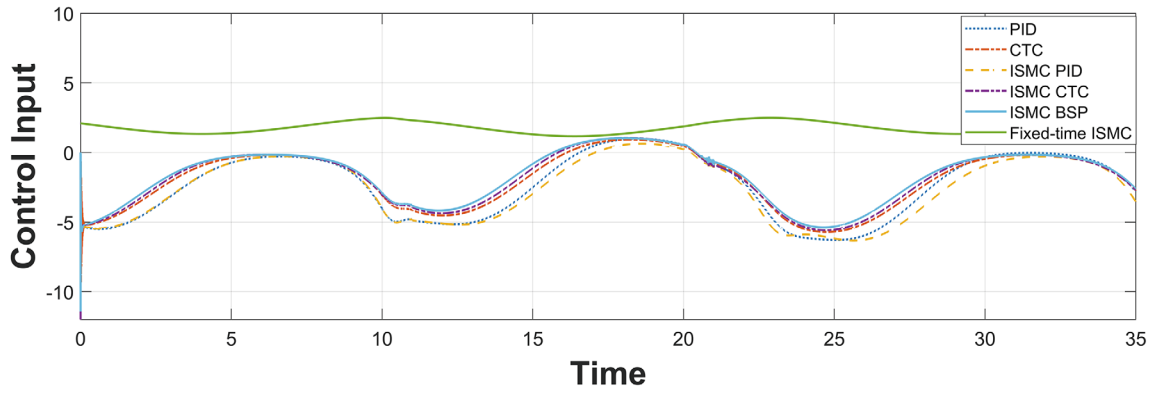

FIGURE 10 Control input for joint 2.

5 | CONCLUSIONS

In this article, a fixed-time ISMC controller based on admittance control has been proposed for robot manipulators such that the robot can comply with the external human forces rather than reject them as disturbances. Furthermore, the convergence time of the system can be predefined regardless of the initial conditions. The simulation results show that the proposed controller can track the reference trajectory precisely with faster convergence of the tracking error. In future work, a fixed-time force observer of external human forces will be discussed and integrated into the system. Safety constraints of the system will also be considered. The whole system will be tested on a robotics platform such as the Baxter robot to further validate the controller's effectiveness and evaluate real-world performance.

ACKNOWLEDGEMENTS

This work was supported in part by the Natural Environment Research Council, United Kingdom under Grant NE/V008080/1, in part by the Royal Society under Grant IEC/NSFC/211236 and Grant RGS/R1/221356, and in part by the U.K. EPSRC Made Smarter Innovation (MSI) - Research Centre for Smart, Collaborative Industrial Robotics under Grant EP/V062158/1.

CONFLICT OF INTEREST STATEMENT

The authors declare no potential conflict of interests.

DATA AVAILABILITY STATEMENT

The data that support the findings of this study are available from the corresponding author upon reasonable request.

ORCID

Yuzhu Sun https://orcid.org/0000-0002-4776-592X

REFERENCES

1. Sharifi M, Azimi V, Mushahwar VK, Tavakoli M. Impedance learning-based adaptive control for human-robot interaction. *IEEE Trans Control Syst Technol*. 2022;30(4):1345-1358.
2. He W, Xue C, Yu X, Li Z, Yang C. Admittance-based controller design for physical human–robot interaction in the constrained task space. *IEEE Trans Autom Sci Eng*. 2020;17(4):1937-1949.
3. Tee KP, Yan R, Li H. Adaptive admittance control of a robot manipulator under task space constraint. *2010 IEEE International Conference on Robotics and Automation*. IEEE; 2010:5181-5186.
4. Okunev V, Nierhoff T, Hirche S. Human-preference-based control design: Adaptive robot admittance control for physical human-robot interaction. *2012 IEEE RO-MAN: The 21st IEEE International Symposium on Robot and Human Interactive Communication*. IEEE; 2012:443-448.
5. Huang L, Ge SS, Lee TH. An adaptive impedance control scheme for constrained robots. *Int J Comput Syst Signals*. 2004;5:17-26.
6. Tsumugiwa T, Yokogawa R, Hara K. Variable impedance control based on estimation of human arm stiffness for human-robot cooperative calligraphic task. *Proceedings 2002 IEEE International Conference on Robotics and Automation (Cat. No. 02CH37292)*. IEEE; 2002:644-650.
7. Chan S, Yao B, Gao W, Cheng M. Robust impedance control of robot manipulators. *Int J Robot Autom*. 1991;6(4):220-227.
8. Liu G, Goldenberg AA. Robust hybrid impedance control of robot manipulators. *Proceedings. 1991 IEEE International Conference on Robotics and Automation*. IEEE Computer Society; 1991:287-288.
9. Zuo Z. Non-singular fixed-time terminal sliding mode control of non-linear systems. *IET Control Theory Appl*. 2015;9(4):545-552.
10. Van M. Adaptive neural integral sliding-mode control for tracking control of fully actuated uncertain surface vessels. *Int J Robust Nonlinear Control*. 2019;29(5):1537-1557.
11. Xu JX, Guo ZQ, Lee TH. Design and implementation of integral sliding-mode control on an underactuated two-wheeled mobile robot. *IEEE Trans Ind Electron*. 2014;61(7):3671-3681. doi:10.1109/tie.2013.2282594
12. Liu Y, Li H, Lu R, Zuo Z, Li X. An overview of finite/fixed-time control and its application in engineering systems. *IEEE/CAA J Automat Sinica*. 2022;9(12):2106-2120. doi:10.1109/jas.2022.105413
13. Yang C, Jiang Y, He W, Na J, Li Z, Xu B. Adaptive parameter estimation and control design for robot manipulators with finite-time convergence. *IEEE Trans Ind Electron*. 2018;65(10):8112-8123.
14. Zuo Z, Tie L. Distributed robust finite-time nonlinear consensus protocols for multi-agent systems. *Int J Syst Sci*. 2016;47(6):1366-1375.
15. Huang S, Wang J. Robust fixed-time integral sliding mode control of a nonlinear hydraulic turbine regulating system. *J Comput Nonlinear Dyn*. 2020;15(3):031002.
16. Li B, Zhang H, Xiao B, Wang C, Yang Y. Fixed-time integral sliding mode control of a high-order nonlinear system. *Nonlinear Dyn*. 2021;107:909-920.
17. Wang JB, Liu CX, Wang Y, Zheng GC. Fixed time integral sliding mode controller and its application to the suppression of chaotic oscillation in power system. *Chinese Phys B*. 2018;27(7):070503.
18. Shi S, Gu J, Xu S, Min H. Globally fixed-time high-order sliding mode control for new sliding mode systems subject to mismatched terms and its application. *IEEE Trans Ind Electron*. 2020;67(12):10776-10786.
19. Feng Y, Yu X, Man Z. Non-singular terminal sliding mode control of rigid manipulators. *Automatica*. 2002;38(12):2159-2167.
20. Yang L, Yang J. Nonsingular fast terminal sliding-mode control for nonlinear dynamical systems. *Int J Robust Nonlinear Control*. 2011;21(16):1865-1879.
21. Zuo Z. Nonsingular fixed-time consensus tracking for second-order multi-agent networks. *Automatica*. 2015;54:305-309.
22. Van M, Ceglarek D. Robust fault tolerant control of robot manipulators with global fixed-time convergence. *J Franklin Ins*. 2021;358(1):699-722.

23. Cao WJ, Xu JX. Nonlinear integral-type sliding surface for both matched and unmatched uncertain systems. *IEEE Trans Autom Control*. 2004;49(8):1355-1360. doi:10.1109/TAC.2004.832658
24. Zhang L, Wang Y, Hou Y, Li H. Fixed-time sliding mode control for uncertain robot manipulators. *IEEE Access*. 2019;7:149750-149763. doi:10.1109/ACCESS.2019.2946866
25. Rubagotti M, Estrada A, Castanos F, Ferrara A, Fridman L. Integral sliding mode control for nonlinear systems with matched and unmatched perturbations. *IEEE Trans Autom Control*. 2011;56(11):2699-2704. doi:10.1109/TAC.2011.2159420
26. Li H, Cai Y. On SFTSM control with fixed-time convergence. *IET Control Theory Appl*. 2017;11:766-773.
27. Van M, Sun Y, Mcllvanna S, Khyam M, Ceglarek D. Adaptive fuzzy fault tolerant control for robot manipulators with fixed-Time convergence.
28. Craig JJ, Hsu P, Sastry SS. Adaptive control of mechanical manipulators. *Int J Robotics Res*. 1987;6(2):16-28.

How to cite this article: Sun Y, Van M, McIlvanna S, McLoone S, Ceglarek D. Fixed-time integral sliding mode control for admittance control of a robot manipulator. *Int J Robust Nonlinear Control*. 2024;34(5):3548-3564. doi: 10.1002/rnc.7150